Nuclear Instruments and Methods in Physics Research A285 (1989) 211–216
North-Holland, Amsterdam

3D PARTICLE SIMULATION AND 3D LINEAR MODEL ANALYSIS OF FELIX

R.W.B. BEST, B. FAATZ, D. OEPTS and P.W. VAN AMERSFOORT

Instituut voor Plasmafysica "Rijnhuizen", Ass. Euratom – FOM, Edisonbaan 14, 3439 MN Nieuwegein, The Netherlands

E. JERBY

Faculty of Engineering, Tel-Aviv University, Ramat-Aviv, 69978, Israel

T.-M. TRAN

CRPP, Ass. Euratom – CS, ÉPFL, 21 Av. des Bains, 1007 Lausanne, Switzerland

For the design of the Dutch free electron laser FELIX [P.W. van Amersfoort et al., this issue] computer simulations are done with two different codes, G3DH and TDA, to estimate three dimensional effects in the amplification process in the undulator. G3DH [E. Jerby and A. Gover, Nucl. Instr. and Meth. A272 (1988) 380] solves a 3D matrix gain dispersion equation, TDA [T.-M. Tran and J.S. Wurtele, to be published] is a nonlinear 3D particle simulation code. Both codes take into account energy spread and emittance of the electron beam, Rayleigh length and waist position of the e.m. beam, and the planar undulator form. The finite length of the electron beam microbunches is not considered. The two methods to calculate the evolution of the beam profiles along the undulator are compared. Beam guiding and other effects are presented for various input conditions.

1. Introduction

The Dutch Free Electron Laser for Infrared eXperiments (FELIX) project involves the construction of a rapidly tunable FEL. Calculations have been done [1] based on a 1D analysis, mainly to define the required beam parameters for the electron linac. In order to optimize the design of the optical cavity it is necessary to take into account 3D effects like beam guiding. Results obtained with two different computer simulation methods are described in the next sections. These 3D simulations do not (yet) take into account the finite length of the electron micropulses. This is done in a 1D simulation [12].

2. Particle simulation

The Three-Dimensional Axisymmetric (TDA) model of Tran and Wurtele [3] is based on the following assumptions to simplify the equations of motion for the beam electrons and the wave equations for the field potentials.

Space charge effects are neglected. This eliminates the scalar potential. The axial component of the vector potential is chosen to be zero. The transverse components of the dimensionless vector potential $a = eA/mc$ of the e.m. beam are cast in the eikonal form $a_s(r, z)\, e^{i\Phi_s(r,z)}\, e^{ik_s(z-ct)}$, independent of the cylindrical coordinate φ, and with $k_s \gg \partial_z \ln a_s$, $\partial_z \ln \phi_s$. This form eliminates ∂_φ, ∂_z^2 and ∂_t^2 terms in the left hand side of the wave equation (5), which is shown below.

The e.m. beam is supposed to have a fundamental Gaussian form [4] with spot size s and wave front curvature R before the electron beam enters:

$$a_s\, e^{i\Phi_s} = a_{s0}\frac{s_0}{s(z)}\exp\left(\frac{-r^2}{s^2(z)}\right) \times \exp\left(i\zeta(z) + i\frac{k_s r^2}{2R(z)}\right), \tag{1}$$

in which

$$s^2 = s_0^2\left[1 + (z - z_0)^2/l_R^2\right],$$

$$\tan\zeta = (z - z_0)/l_R$$

and

$$R = (z - z_0) + l_R^2/(z - z_0)$$

in terms of the waist position z_0 and the Rayleigh length $l_R = k_s s_0^2/2$, s_0 being the minimum spot size. Eq. (1) satisfies eq. (5) with zero right hand side.

TDA can handle e.m. pump waves and magnetostatic wigglers, but here only the latter are considered. A helical wiggler excites a circularly polarized wave.

The potential of wiggler and wave reads

$$a_x - \mathrm{i}a_y = -a_w(x, y)\,\mathrm{e}^{-\mathrm{i}k_w z} + a_s\,\mathrm{e}^{\mathrm{i}\phi_s}\,\mathrm{e}^{\mathrm{i}k_s(z-ct)}. \quad (2)$$

A planar wiggler excites a linearly polarized wave. Then e.g., $a_x = 0$ and a_y equals the real part of the right hand side of eq. (2).

Electron motion is described by a set of six ordinary differential equations for the Lorentz factor γ, the phase $\theta = k_w z + k_s z - k_s ct$, the coordinates x and y, and the dimensionless generalized momenta $\rho_x = P_x/mc$ and $\rho_y = P_y/mc$. The independent variable is z, so $t = t(z)$. It is assumed that $\gamma \gg 1$ and $a_s \ll a_w$.

The six equations are averaged over a wiggler period. The averaged electron motion proves to depend on the wiggler potential only through its modulus squared and averaged over a wiggler period. Henceforth a_w denotes this rms value. For a helical wiggler a_w depends on r only.

In a planar wiggler electrons are periodically detuned: the phase θ has, in addition to its slow variation, a term $\xi \cos 2k_w z$ with $\xi = a_w^2(0, 0)/2(a_w^2(0, 0) + 1)$ [5]. This term results, upon averaging of the equations of motion, in a decoupling factor $f_B = J_0(\xi) - J_1(\xi)$ with Bessel functions J_0 and J_1. For a helical wiggler $f_B = 1$.

With these assumptions the equations of motion reduce to the set (a prime denotes $\mathrm{d}/\mathrm{d}z$)

$$\gamma' = -k_s a_w a_s f_B \sin(\theta + \phi_s)/\gamma,$$
$$\theta' = \mu + k_s a_w a_s f_B \cos(\theta + \phi_s)/\gamma^2, \quad (3)$$

where

$$\mu = k_w - k_s\left(1 + a_w^2 + \rho_x^2 + \rho_y^2\right)/2\gamma^2$$

is the detuning parameter, and

$$x' = \rho_x/\gamma, \qquad \rho_x' = -\partial_x\left(a_w^2\right)/2\gamma,$$
$$y' = \rho_y/\gamma, \qquad \rho_y' = -\partial_y\left(a_w^2\right)/2\gamma. \quad (4)$$

TDA solves this set for each electron, together with the complex partial differential equation for the field. In the wave equation

$$\left(\frac{1}{r}\partial_r r\,\partial_r + 2\mathrm{i}k_s\,\partial_z\right)a_s\,\mathrm{e}^{\mathrm{i}\phi_s} = -\frac{4\pi}{I_A}f_B\left\langle a_w j\frac{\mathrm{e}^{-\mathrm{i}\theta}}{\gamma}\right\rangle \quad (5)$$

r, φ and t are independent variables in addition to z, but the φ and t dependences are averaged out, indicated by angle brackets (cf. ref. [6]). The current density $j(x, y, z, t)$ is derived from the total current I and the x and y positions of the electrons, neglecting velocity differences. $I_A = 17$ kA is the Alfvén current.

3. Matrix gain–dispersion solution

The G3DH computer code is based on a generalized, linear, three-dimensional model of the FEL amplifier [2,7,8,10]. This 3D model is represented by the matrix gain–dispersion equation

$$\boldsymbol{E}_X(s) = \left\{[\mathbf{I} + \mathbf{R}\chi_z]\cdot\mathbf{K}(s) - \mathrm{i}\kappa\mathbf{G}\chi_z\right\}^{-1}\cdot[\mathbf{I} + \mathbf{R}\chi_z]\cdot\hat{\boldsymbol{E}}_{X0}(z = 0), \quad (6)$$

where s is the Laplace variable, defined by $\mathbf{L}\{a(z)\} = \tilde{a}(s) = \int_{z=0}^{\infty} a(z)\exp(-sz)\,\mathrm{d}z$. Each component of the e.m. field vectors, $\boldsymbol{E}_X(s)$ and $\hat{\boldsymbol{E}}_{X0}(z = 0)$, represents a transverse spatial Fourier component of the radiation wave at the exit of and at the entrance to the interaction region, respectively. Using either periodic or vanishing field boundary conditions in the transverse dimensions ($x = \pm a$, $y = \pm b$) the free-space transverse modes and the corresponding components of the vectors $\boldsymbol{E}_X(s)$ and $\hat{\boldsymbol{E}}_{X0}(z = 0)$ are characterized by mode indices (n, m), and axial wavenumbers

$$k_{z_{nm}} = \sqrt{k^2 - k_{\perp_{nm}}^2}.$$

The unit matrix is denoted as $\mathbf{I}$. $\mathbf{K}(s)$ is a diagonal matrix that represents the e.m. wave propagation constants for the various vacuum modes. Its diagonal terms are $(s^2 + k_{z_{nm}}^2)/2s$. The matrix $\mathbf{G}$ is the e-beam coupling matrix. It consists of the transverse spatial Fourier components of e-beam profile function,

$$\bar{g}_{mn} = \int_{-a}^{a}\int_{-b}^{b} g_0(x, y)\exp(\mathrm{i}mk_{0x}x + \mathrm{i}nk_{0y}y)\,\mathrm{d}x\,\mathrm{d}y.$$

The space-charge reduction matrix is [7]

$$\mathbf{R} = -\frac{\omega^2}{2\left\langle\gamma_z^2\bar{v}_z^2\right\rangle(s + \mathrm{i}k_w)}\mathbf{G}\cdot\left[\mathbf{K}(s + \mathrm{i}k_w)\right]^{-1}. \quad (7)$$

The longitudinal susceptibility of the electron beam inside the wiggler is given by

$$\chi_z = -\frac{\mathrm{i}e^2}{\epsilon_0\omega}\int_{\bar{p}_z=-\infty}^{\infty}\frac{\partial f(\bar{p}_z)/\partial\bar{p}_z}{s + \mathrm{i}k_w - \mathrm{i}\omega/\bar{v}_z}\,\mathrm{d}\bar{p}_z, \quad (8)$$

where $f(\bar{p}_z)$ is the e-beam distribution function and $\bar{p}_z = \gamma m\bar{v}_z$ is the longitudinal momentum of the electrons. The general kinetic definition of the susceptibility function χ_z permits to take into consideration all the quality degradation factors of the e-beam. The normalized distribution function that incorporates the effects of the emittance, the transverse magnetic field gradient and the energy spread on the axial velocity spread is [8] $f_u(u) = U\exp[U(U + u)]\,\mathrm{erfc}(U + u)$. The normalized variable is defined as $u \equiv (\bar{v}_z - \bar{v}_{0z})/(\bar{v}_{0z}\delta_\gamma)$ and the factor U is given by $U = \lambda_\beta\delta_\gamma/2\epsilon_b$. The axial velocity spread due to the energy spread contribution $\delta_\gamma = \Delta\gamma/\gamma_{0z}^2\gamma_0$, the emittance is $\epsilon_b = \pi r_b\,\Delta\phi$, and the period of the betatron motion is λ_β. The susceptibility integral is [8]

$$\chi_z = \frac{\theta_p^2}{\left(\theta_{th}^{es}\right)^2}2U\int_{y=0}^{\infty}\mathrm{e}^{-2Uy}Z'\left(\zeta(s + \mathrm{i}k_w) + y\right)\mathrm{d}y, \quad (9)$$

where the FEL constitutive parameters [9] are the space-charge parameter $\theta_p = \omega_p'/\bar{v}_{0z}$ (ω_p' is the longitudinal relativistic plasma frequency on axis) and the detuning spread parameter (due to energy spread) $\bar{\theta}_{th}^{es} = (\omega/\bar{v}_{0z})\delta_\gamma$. The complex error function is $Z'(z)$ and its argument in eq. (9) includes a complex variable, given by $\zeta(s) = (i\omega/\bar{v}_{0z} - s)/s\delta_\gamma$.

The coupling parameter κ is defined as

$$\kappa = \frac{\omega V_{Wx}^2 f_B^2}{8c^2\langle \bar{v}_z \rangle}, \tag{10}$$

where V_{Wx} is the amplitude of the wiggling motion velocity. The gain matrix, $\kappa \mathbf{G}\chi_z$, measures the strength of the FEL interaction. Its diagonal terms describe the coupling of each vacuum mode with itself and the off-diagonal terms measure the coupling between the different modes due to the FEL mode coupling mechanism.

The order of the 3D matrix equation, i.e. the number of angular spectrum components that are needed to properly describe the FEL interaction, can be determined by various practical considerations summarized in ref. [2]. Typically, ten angular spectral components are needed to properly describe each transverse dimension. Hence, the matrix equation is of order 100 and can be easily solved by standard library subroutines for complex matrices inversion.

Following the numerical steps, an inverse Laplace transform is applied to solve the matrix gain–dispersion equation (6). This results in a vector that consists of spatial Fourier components of the field at a given distance z. The components can now be summed up as an inverse discrete Fourier transform to yield the e.m. field complex profile $E(x, y, z) = \mathbf{L}^{-1}\{\Sigma_{\mathbf{k}_\perp} E(\mathbf{k}_\perp, s)\, e^{i\mathbf{k}_\perp \cdot \mathbf{x}_\perp}\}$ producing the evolution of the fields in space.

4. Results

For the simulation of FELIX [1] the following parameter values are used. For all figures these values apply, unless stated otherwise. Wiggler: period $2\pi/k_w = 65$ mm, length 38 periods = 2.47 m, parameter $a_w = 1 + \frac{1}{2}k_w^2 r^2$. Electron beam at wiggler entrance: Gaussian γ distribution with average 50 and standard deviation 0.125, current $I = 70$ A, radius 0.38 mm, normalized emittance 50π mm mrad. E.m. beam wavelength $2\pi/k_s \approx 26$ μm, adjusted for maximum gain.

Figs. 1–5 show results of TDA runs. The wiggler is assumed to be helical ($f_B = 1$). The Rayleigh length l_R is 1.69 m, corresponding to $s_0 = 3.7$ mm. The waist position z_0 is 1.85 m except for fig. 3. Results are insensitive to the input power (1 W–100 kW) except for figs. 2 and 3. The shape of the gain curve in fig. 1 agrees

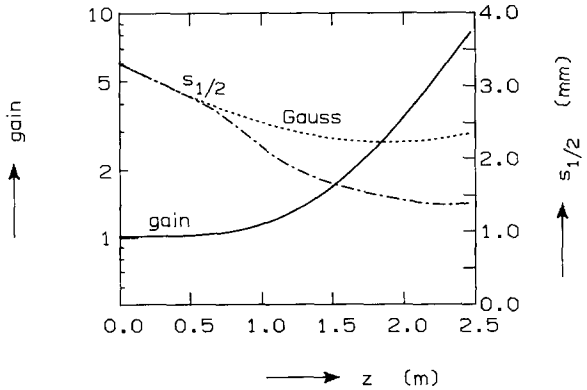

Fig. 1. Particle simulation (TDA). Gain and spotsize $s_{1/2}$ as a function of distance z along the wiggler. Without FEL interaction $s_{1/2}$ would follow the Gauss curve (see section 4).

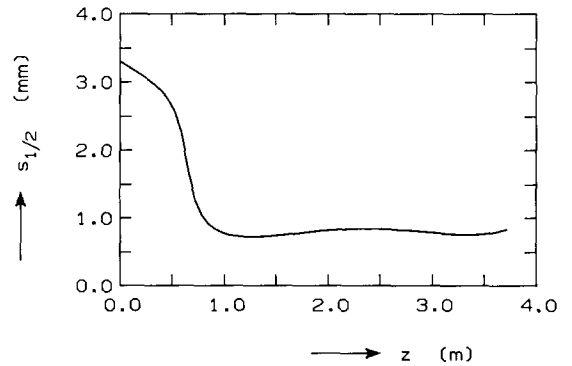

Fig. 2. Particle simulation (TDA). Spotsize $s_{1/2}$ as a function of distance along the wiggler at very high current. The e.m. beam is guided by betatron oscillations (see section 4).

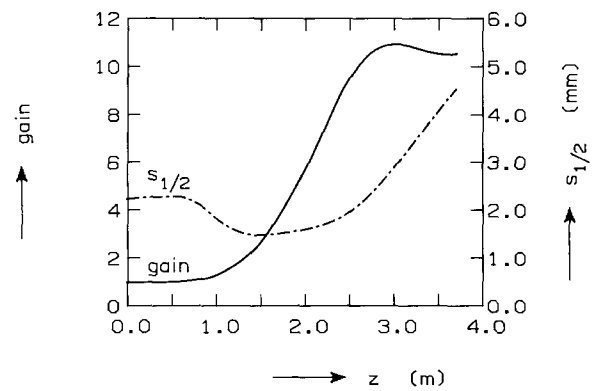

Fig. 3. Particle simulation (TDA). Gain and spotsize $s_{1/2}$ as a function of distance along the wiggler. Gain saturation and loss of guiding at high power (see section 4).

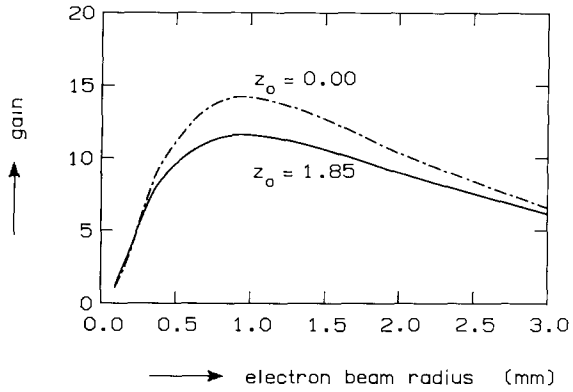

Fig. 4. Particle simulation (TDA). Gain as a function of electron beam radius, for two waist positions z_0 of the incident e.m. beam (see section 4).

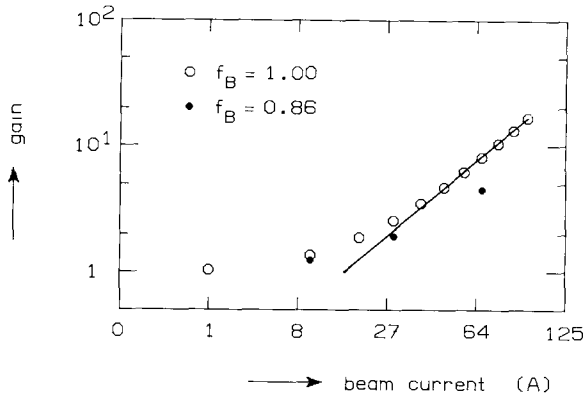

Fig. 5. Particle simulation (TDA). Gain as a function of electron beam current, for helical ($f_B = 1$) and planar ($f_B = 0.86$) wiggler. Asymptotic behaviour at high current (see section 4).

roughly with 1D theory (cf. fig. 4 in ref. [11]). The spotsize $s_{1/2}$ is the radius which contains half of the e.m. power. For a Gaussian (1) $s_{1/2} = 0.59s$. The deviation from the hyperbolic form of $s(z)$ indicates *beam guiding*. This is more evident in fig. 2 in which the wiggler length is 3.7 m, the electron beam radius at entrance is 1 mm and the current is 484 A. The e.m. beam follows the *betatron oscillations* (due to mismatch) of the electron beam. The oscillation period (2.3 m) is approximately determined by $x'' = -\frac{1}{2}(a_w k_w/\gamma)^2 x$ which follows from eq. (4) for constant γ. The nonlinear character of TDA is seen in fig. 3 which shows saturation of an e.m. beam with 2.25 MW power at wiggler entrance. The wiggler length is 3.7 m, the waist position z_0 is 0 and the normalized emittance is 10π mm mrad. Note that beam guiding disappears at saturation. Fig. 4 plots the gain against the electron beam radius at entrance, for two waist positions z_0. Maximum gain is reached for 1 mm radius. Fig. 5 shows the

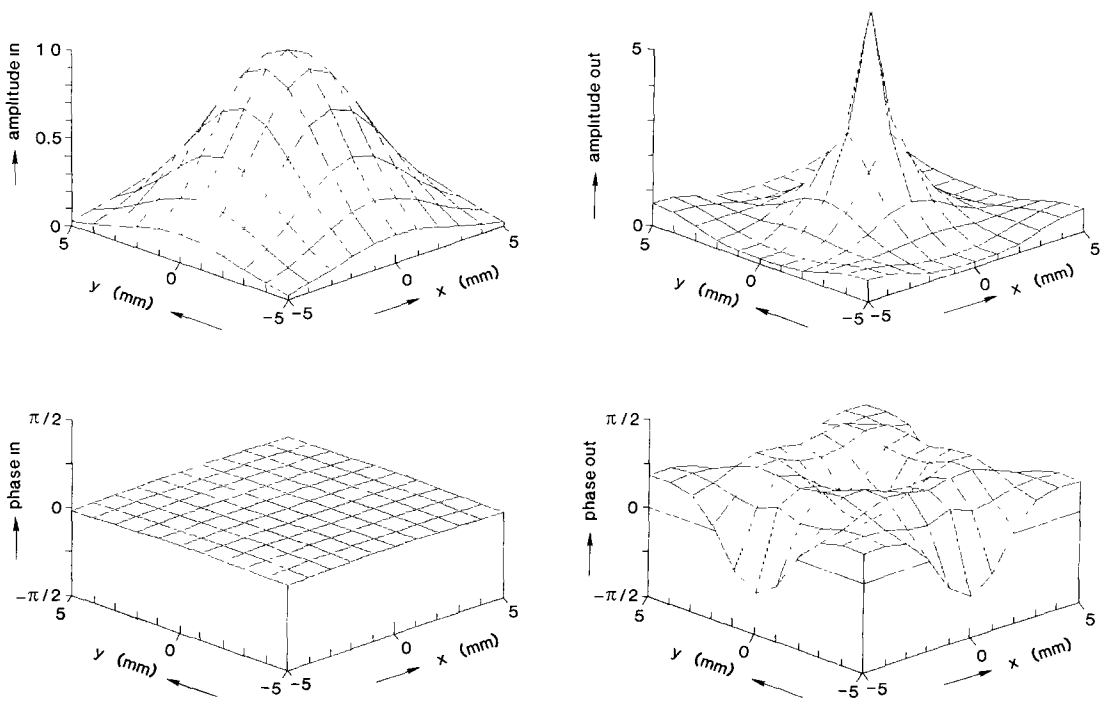

Fig. 6. Dispersion equation (G3DH). Amplitude and phase profile, at wiggler entrance (left) and exit (right). Incident beam is focused at entrance. Gain = 5.5 (see section 4).

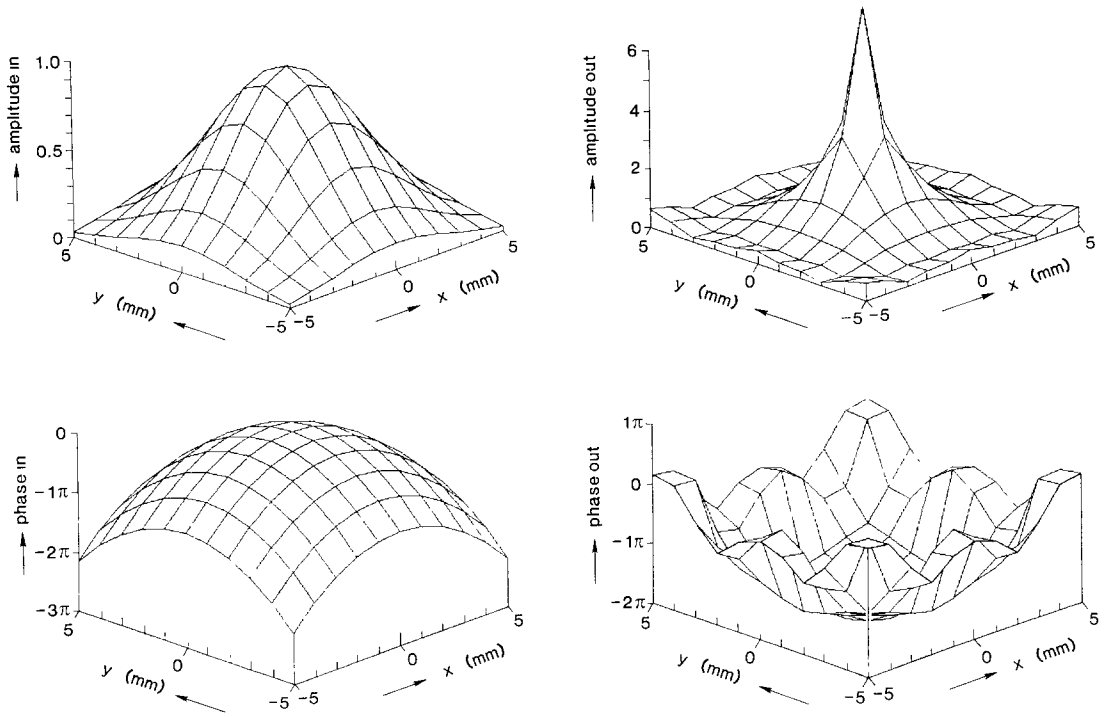

Fig. 7. Dispersion equation (G3DH). Amplitude and phase profile at wiggler entrance (left) and exit (right). Radius of curvature of incident e.m. beam is 0.9 m. Gain = 7.2 (see section 4).

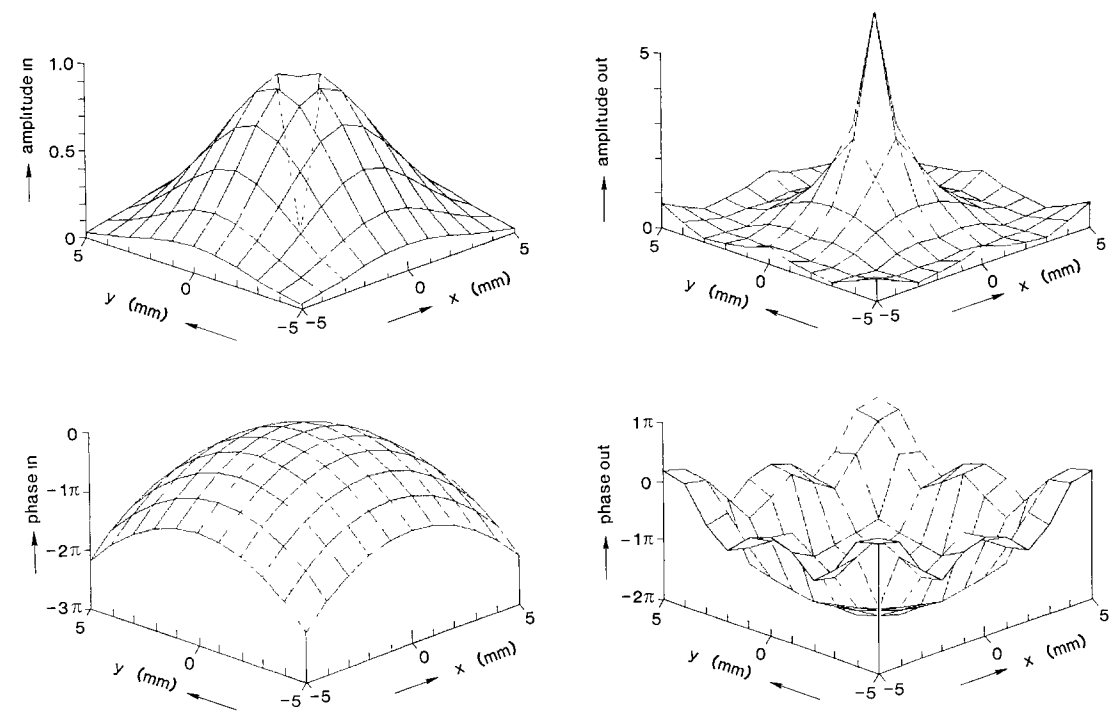

Fig. 8. Dispersion equation (G3DH). Amplitude and phase profile, at wiggler entrance (left) and exit (right). Radius of curvature of incident e.m. beam is 0.9 m. Dip at entrance has recovered at exit. Gain = 5.6 (see section 4).

asymptotic behaviour of the gain for increasing current, an exponential function of $I^{1/3}$ as expected from theory [9]. The three black dots show the reduced gain for $f_B = 0.86$, the correction factor for a planar wiggler with $a_w = 1$ (rms value). For the standard value $I = 70$ A the gain is 5.0.

Figs. 6–8 show results of G3DH runs. The planar wiggler form for FELIX is taken into account. Arbitrary units are used along the a axis. In fig. 6 the waist of the e.m. beam is put at wiggler entrance hence the flat phase profile. The spotsize s_0 is 3.7 mm. Beam guiding is evident from the amplitude profile at wiggler exit; the gain is 5.5. In fig. 7 the radius of curvature $R(0)$ is optimized keeping the spotsize $s(0)$ constant at 3.7 mm. The maximum gain of 7.2 is reached for $R(0) = 0.9$ m. In fig. 8 the same entrance conditions as in fig. 7 are used except for one point: the e.m. wave amplitude is set equal to 0 on axis. Such a dip can occur when a mirror is used with a hole in the center for the electron beam (to avoid bending magnets). The amplitude profile has recovered at wiggler exit, but the gain drops to 5.6.

5. Comparison

G3DH and TDA are different in almost every respect. G3DH solves the linearized Vlasov equation, 3D in space and 1D in momentum, as a boundary value problem using Laplace transform in z and Fourier transform in x, y. TDA calculates 3D electron trajectories and solves a 2D wave equation in r, z. G3DH uses analytical expressions for the betatron motion to find the electron beam profile. A major issue is the convolution operation between the Fourier spectra of the electron beam and the e.m. beam. TDA calculates nonlinear axial pendulum motion, so bunching and saturation effects are included. G3DH treats betatron motion, emittance and energy spread as independent random causes of spread and skewness of the axial velocity distribution. In this linear model only the onset of axial bunching is included (which does not exclude high gain). TDA ignores space charge, G3DH includes it.

In spite of their very different setup, the two codes yield similar results in the regime in which FELIX is to work. As mentioned in the previous section, the gain is around 5 if the microbunches are long. According to 1D theory [1,12] the gain would be 2.1 under the same conditions. So it appears that the various assumptions which underlie the 3D simulations are justified, and that 3D effects are important.

Acknowledgements

This work was performed with financial support from the "Nederlandse Organisatie voor Wetenschappelijk Onderzoek" (NWO) and Euratom. One of us (B.F.) gratefully acknowledges a Shell grant to attend this Conference.

References

[1] P.W. van Amersfoort et al., these Proceedings (10th Int. Free Electron Laser Conf., Jerusalem, Israel, 1988) Nucl. Instr. and Meth A285 (1989) 67.
[2] E. Jerby and A Gover, Proc. 9th Int. FEL Conf, Williamsburg, 1987, Nucl. Instr. and Meth. A273 (1988) 380.
[3] T -M. Tran and J.S Wurtele, to be published. J. Comput. Phys.
[4] A. Yariv, Introduction to Optical Electronics (Holt, Rinehart and Winston, 1971).
[5] W.B. Colson, IEEE J. Quantum Electron. QE-17 (1981) 1417.
[6] N.M. Kroll, P.L. Morton and M.N. Rosenbluth, IEEE J. Quantum Electron. QE-17 (1981) 1436.
[7] E Jerby, Ph.D. thesis, to be published
[8] E. Jerby, Proc. 9th Int FEL Conf., Williamsburg, 1987, Nucl. Instr. and Meth. A272 (1988) 457
[9] E. Jerby and A. Gover, IEEE J. Quantum Electron. QE-21 (1985) 1041
[10] E. Jerby and A. Gover, these Proceedings (10th Int Free Electron Laser Conf., Jerusalem, Israel, 1988) Nucl Instr and Meth. A285 (1989) 128.
[11] C.-C. Shih, A Yariv, IEEE J Quantum Electron. QE-17 (1981) 1387.
[12] D. Oepts et al., these Proceedings (10th Int Free Electron Laser Conf, Jerusalem, Israel, 1988) Nucl. Instr. and Meth. A285 (1989) 204